Available online at www.sciencedirect.com

ScienceDirect

Energy Procedia 101 (2016) 1143 – 1150

Energy Procedia

71st Conference of the Italian Thermal Machines Engineering Association, ATI2016, 14-16 September 2016, Turin, Italy

Scale Adaptive Simulations of a swirl stabilized spray flame using Flamelet Generated Manifold

Stefano Puggelli*, Davide Bertini, Lorenzo Mazzei, Antonio Andreini

Department of Industrial Engineering, University of Florence, Via S. Marta 3, Firenze – 50139, Italy

Abstract

The present work describes the main findings derived from CFD simulations of the swirl stabilized spray flame experimentally investigated by Sheen [1]. Scale Adaptive Simulations (SAS) have been performed using Flamelet Generated Manifold (FGM) for combustion modelling and a Eulerian-Lagrangian approach for liquid phase description. Results highlight the capabilities of SAS in predicting the main characteristics of the analysed turbulent spray flame, leading to appreciable enhancements with respect to RANS results in terms of both velocity and temperature distributions.

Peer-review under responsibility of the Scientific Committee of ATI 2016.

Keywords: CFD; turbulent combustion; spray flame; SAS; FGM.

1. Introduction

Lean burn combustion is one of the most promising technologies for the reduction of NOx emissions imposed by ICAO-CAEP [2]. Its implementation in common aero-engines is related to several technological issues, among which it is worth mentioning flame blow-off, limited availability of coolant and thermoacoustics instabilities. Considering the costs and the complexity related to experimental investigations at high pressure and temperature, CFD methods are of primary importance to better understand all the phenomena involved.

* Corresponding author. Tel.: +39-055-2758772.
E-mail address: stefano.puggelli@htc.de.unifi.it

Peer-review under responsibility of the Scientific Committee of ATI 2016.
doi:10.1016/j.egypro.2016.11.155

Scale-Resolved Simulations in particular are capable of overcoming the limitations of classical RANS approaches, which seem to be unable or insufficient to represent the physical complexity of lean combustors [3]. Indeed, Large Eddy Simulation (LES) and hybrid RANS-LES models (e.g. Detached Eddy Simulation (DES) or Scale Adaptive Simulation (SAS)) have been already successfully applied for the simulation of both premixed and non-premixed gaseous flames [4–6]. Recently, researchers have shown also their suitability for the simulation of reactive multiphase flows, mainly for laboratory test conditions [7,8].

As far as the combustion modelling is concerned, in order to correctly catch the complex topology normally shown by the flame in lean combustors, approaches characterized by a detailed description of the kinetic mechanisms are required. To this end, Flamelet Generated Manifold (FGM) model, where a pre-computed laminar flamelet solution is weighted through a pre-defined probability density function (PDF) in order to account for flame turbulent wrinkling, has proved to accurately describe the flame evolution since it can locally take into account finite rate and non-equilibrium effects [7,9]. Moreover, in order to properly catch the evolution of the two phase flow under investigation, a Eulerian-Lagrangian strategy can be used for the coupling between the gas and the liquid phase, allowing a straightforward implementation of physical processes such as evaporation or secondary break-up.

In a previous work of same authors [10], capabilities of SAS approach for describing unsteady and interacting features of a turbulent reacting two-phase flow have been showed and some limitations of tabulated chemistry approaches, such as FGM, proved. However, deeper comparison and more detailed experimental data than the ones available in [10] would have been required to clearly appreciate the effects and limits of combustion modelling.

In the present work, Scale Adaptive Simulations of the swirl stabilized spray flame experimentally investigated in [1] have been performed using Flamelet Generated Manifold for combustion modelling and an Eulerian-Lagrangian approach for liquid phase description. The chosen test case consists of an annular air channel fed by a single axial swirler that ends in a tubular liner. Liquid kerosene is injected by a pressure atomizer located at the liner inlet plane along the channel axis. Burner operates at ambient pressure and burning conditions are typical of partially premixed lean flames with a global equivalence ratio close to the blowout limit. It has been chosen since detailed measurements of velocity, temperature and main species fields are available on radial planes at several axial distances from the inlet giving the chance to assess the characteristics of the chosen numerical models. Obtained results in scale resolved framework have been compared with the available experimental data and with steady state solutions. The commercial code ANSYS Fluent v16.2 has been employed in the present work, which have been performed exploiting CINECA High Performance Computing (HPC) clusters.

Nomenclature

c	Normalized progress variable [-]
D_0	Diameter of the combustion chamber [m]
D_{in}	Inner diameter of the annular duct [m]
D_{out}	Outer diameter of the annular duct [m]
L_{vk}	Von Karman length scale [m]
MFR	Mass flow rate [g/s]
q	Spread parameter of Rosin Rammler distribution [-]
SMD	Sauter Mean Diameter [m]
S	Swirl number [-]
T	Temperature [K]
R	Inner radius of the annular duct [m]
V	Velocity [m/s]
Z	Mixture fraction [-]
Y	Species mass fraction [-]

Greek

Θ	Cone injection spray angle [°]

Acronyms

CFD	Computational Fluid Dynamics
CAEP	Committee on Aviation Environmental Protection
DES	Detached Eddy Simulation
FGM	Flamelet Generated Manifold
ICAO	International Civil Aviation Organization
LES	Large Eddy Simulation
PDF	Probability Density Function
RANS	Reynolds Averaged Navier Stokes
rms	Root Mean Square
SAS	Scale Adaptive Simulation
TAB	Taylor Analogy Breakup

2. Modelling

SAS approach represents an improvement of standard URANS formulation based on the introduction of the von Karman length scale L_{vk} into the $k-\omega$ SST turbulence equations in order to dynamically adjust the resolved structures and locally decrease the eddy viscosity [11]. The SAS model stays in RANS mode in zones characterized by low instability, while it switches to a LES behavior in unsteady regions of the flow field. Clearly, if spatial and temporal resolutions are not adequate to correctly catch the turbulent eddies, SAS simulation will permanently remain in RANS mode leading to an overestimation of the eddy viscosity. On the other hand, with respect to DES, this model has proved to be much more robust in terms of computational domain and its numerical effort lower than a complete LES solution. On a mathematical point of view, SAS governing equations differ from those of standard $k-\omega$ SST RANS model only for an additional source term in the ω-equation proportional to the von Karman length scale L_{vk}. The reader interested in such topic is addressed to reference [11], where such model is presented in detail.

Beyond turbulence resolution, combustion modelling is of paramount importance for the proper representation of a turbulent spray flame. In this work, the Flamelet Generated Manifold model has been considered. In FGM a two-dimensional manifold $f(Z,c)$ is generated solving a set of laminar adiabatic one-dimensional flamelets and describing the chemical state and reaction progress space only as function of two control variables, i.e. the mixture fraction Z and the normalized progress variable ($c = Y_c/Y_{ceq}$). In the present work the un-normalized reaction progress variable has been evaluated as:

$$Y_c = Y_{CO} + Y_{CO2}$$

As suggested in [12], a diffusive flamelet behavior has been considered for the test case under investigation and flamelet equations have been solved using the dedicated solver integrated in ANSYS Fluent, generating a set of 64 opposed-jet non-premixed flamelets exploiting the reaction mechanism for $C_{10}H_{22}$ provided in [13] with 100 species and 856 reactions. The interactions between flame and turbulence has been accounted through a Presumed Probability Density Function (PDF) approach, where variances of mixture fraction and progress variable have been modelled through transport equations [10]. In order to include heat losses, due to spray evaporation, an extra dimension due to the filtered enthalpy gain/loss has been added to the tables, while radiative effects have been neglected.

For the dispersed phase modelling a Lagrangian formulation has been adopted. Such approach is suitable when the spray can be described with a dilute assumption and in the test case under investigation such assumption is well satisfied except for the very near injector region. Models for droplet motion, evaporation and heat transfer are needed to obtain spray distribution and provide source terms of mass, momentum and energy to continuous phase. In this work, for the liquid momentum equation, buoyancy and gravity effects have been neglected and the drag coefficient has been evaluated using the hypothesis of spherical not deformable shape droplet. Secondary breakup effects have been accounted through the well-known Taylor Analogy Breakup (TAB) model [14] since the maximum Weber

number inside the computational domain was found to be lower than 100 in all the simulations realized. Moreover, for the evaporation modelling a uniform temperature model has been exploited where the integration of convection contribution on the mass transfer is included exploiting the formulation derived in [15]. Finally, in order to correctly determine the evaporation rate, liquid phase properties of $C_{10}H_{22}$ have been considered as function of both pressure and temperature using data and correlations reported in [16].

3. Description of the test case

The experimental test case investigated in the present study was studied by Sheen [1] and consists of a cylindrical combustion chamber fed by a swirled air jet flowing through an annular duct. A sketch of the experimental domain is depicted in Figure 1, where the main geometrical features are reported. The combustion chamber is 500 mm long, with a diameter D_0 of 200 mm. The annular duct has an inner diameter D_{in} of 21.7 mm and an outer diameter D_{out} of 45.3 mm. The swirler, which provides a tangential component to the air entering the annular duct, is characterized by 20 vanes with a discharge angle of 30°. The fuel injector is located in the center of the combustor (x=0 mm) and injects Jet A-1 through a pressure atomizer with a diameter of 0.25 mm, generating a hollow cone spray. It is worth mentioning that air and fuel entered the combustion chamber at ambient temperature and that all the tests were carried out at atmospheric pressure, as the exit of the burner that is open to the ambient.

Experimental measurements of velocity profiles at isothermal conditions, as well as velocity, temperature and species (O_2, CO_2, CO and H_2) at reactive conditions are available at several axial positions. Measurements were performed only within the combustion chamber, therefore the actual conditions at the exit of the annular duct are not available. In the present work, results just related to the reacting test point are considered for the sake of clarity, but the proposed numerical tools have been validated also in isothermal conditions.

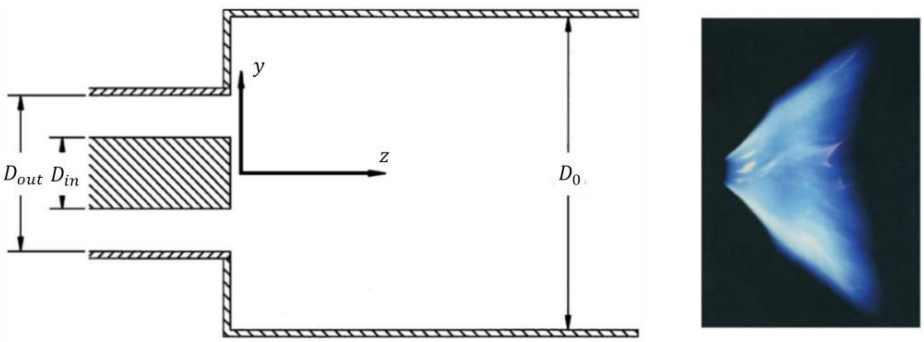

Figure 1: Sketch of the geometry (adapted from [17]) and experimental visualization of the flame [12].

4. Numerical setup

Calculations were carried out on computational grids generated in ANSYS Meshing and reported in Figure 2. A coarse mesh (M1), consisting of 2.8M elements tetrahedrons elements and 0.59M nodes with 5 prism layers for wall modelling and with a size of 2 mm at the annular duct exit, was generated at first. A further refined grid (M2), with a minimum size of 1 mm, was then created for SAS simulations, counting 9.9M elements and 1.8M nodes. On the other hand, RANS simulations have been instead realized on a 90° domain in order to ease the convergence and reduce the computational effort.

From the picture it is possible to notice the inlet (on the left), located upstream of the front plate of the combustor, and the outlet of the domain. Considering the lack of geometrical details for the swirler, coherently with other previous numerical works on the same test case [12,18], it has been not included in the computational domain and its effects are taken into account imposing a swirling velocity component at inlet. Starting from the swirler number value (S_n) reported in [12] and considering an axial velocity component consistent with the experimental mass flow rate, a trial-

and-error procedure has been performed in RANS context to estimate the azimuthal velocity component for a given axial position of the inlet boundary to match the experimental velocity profiles at the first experimental section. For the sake of clarity such sensitivity analysis has not been reported here. Consistently with boundary conditions specified in [19], resulting uniform top-hat profiles has been imposed at inlet and the complete data set of the boundary conditions for the gaseous phase is reported in Table 1. A uniform static pressure value has been imposed at the outlet of the combustion chamber and all the other boundaries have been considered as smooth, no slip and adiabatic walls.

Special attention has been devoted to liquid fuel injection, that in this case corresponds to a hollow wide angle cone (70-80°) and for which experimental data only in terms of injection temperature and velocity were available. Therefore, beginning with values from experimental correlations and assuming a Rosin-Rammler spray distribution [12], a preliminary RANS sensitivity analysis both on Sauter Mean Diameter (SMD) and cone angle has been realized. The final set of spray boundary conditions is reported as well in Table 1.

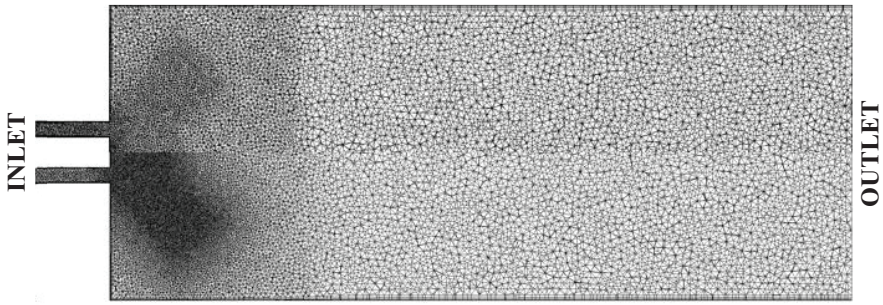

Figure 2: Computational grids M1 (top) and M2 (bottom) used in SAS simulations.

A time step of 5e-6 s has been chosen for SAS simulations with the coarse grid, whereas it has been reduced to 1e-6 s with mesh M2 in order to properly control the Courant number in near injection region and accurately reproduce the main unsteady features of the flow-field. Considering that the geometry under investigation is 0.55 m long and that in reactive test conditions a bulk velocity of 9 m/s is determined, a flow through time of 6.1e-2 s has been considered. Thus, after 2 flow through times required to flush out the initialization and to allow the unsteady flow-field to evolve, statistics were collected on 3 flow-time in order to achieve a statistically representative solution.

In terms of numerical schemes and solution algorithms, in RANS context a coupled algorithm has been employed with second order upwind schemes for spatial discretization, while in SAS framework a PISO algorithm together with bounded central difference schemes for spatial discretization and a second order implicit formulation for time have been used. Finally, for SAS simulations convergence at each time step has been evaluated considering a reduction of three orders of magnitude for residuals of each momentum equation requiring at least 10 iterations per time step.

Table 1: Summary of boundary conditions for liquid and gas phase

	$MFR\ (g/s)$	T (K)	$S_n\ (-)$	SMD (μm)	Θ (°)	q (-)
Gas phase	26.51	300	1.22	-	-	-
Liquid phase	0.951	300	-	64	74	3

5. Results

Figure 3 shows instantaneous and mean temperature and velocity fields obtained in SAS framework with different mesh sizes and with a steady-state approach. The air stream, due to his high tangential component, enters inside the combustion chamber and expands radially creating two main flow structures, i.e. the inner recirculating zone and the corner vortex. The opening angle between steady state and SAS results, considering the averaged data, seems very similar and indeed, even if some major turbulent structures are caught in the near injector region by scale resolved approach, the swirling flow is qualitatively coherent as in RANS simulations. Major discrepancies can be determined

in the corner vortex region where the intensity of the recirculation region, mainly near combustor wall, appears much higher with SAS than in steady simulations. Considering instantaneous results, the proposed mesh refinement in SAS framework leads to catch some smaller turbulent structures and to more physically predict the mixing between spray and swirled flow, even if no appreciable differences have been detected between grids M1 and M2.

On the other hand, considering temperature contours, RANS and SAS results seems quite similar and both simulations predict a physical flame V-shape stabilized immediately after injection region by hot gases recirculation. Temperature peaks are generated at shear layers between the swirled air flow and the main recirculation region leading to high heat releases in the proximity of the injector where a nearly stoichiometric mixture is created. Appreciable differences can be again determined in the corner vortex region, where hot combustion products, due to the stronger recirculation zone predicted in SAS simulations, are convected and some droplets trapped and evaporated creating hot pockets gases. This phenomenon is nearly overlooked in RANS framework that is not completely able to represent such complex swirled flow-field.

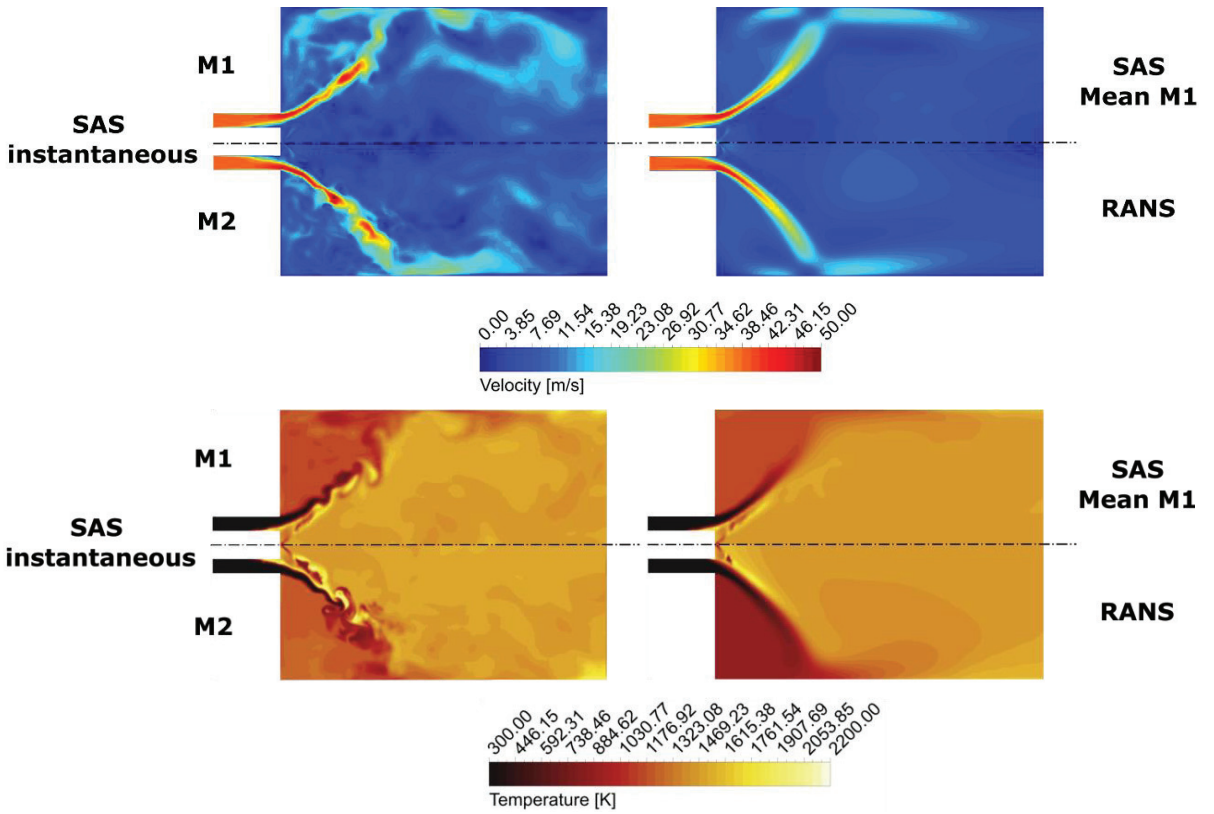

Figure 3: Instantaneous and mean velocity and temperature contours obtained from SAS calculations with several mesh sizes and steady state simulations.

The quantitative comparison between SAS and RANS results against experimental data in terms of velocity and temperature radial profiles at several axial distances (inner radius of the annular duct (R) is used as reference length) is reported in Figure 4. It is worth mentioning that the double peak experimentally detected in axial and radial velocity profiles at the first experimental section is probably generated by the fuel injection. Indeed, in this zone the spray is dense and it is likely that some droplets, interacting with the laser beam, leads to a noise source in the recorded signal [12]. Except this region, in terms of flow field both approaches agree quite well with experimental results and SAS, even if with some minor improvements mainly in terms of axial and radial velocity, is not able to completely recover the opening angle provided by experiments.

Nonetheless, some important differences arise in temperature profiles and are mainly located in the corner vortex region, as previously highlighted about contours. Indeed, SAS is here able to correctly recover the experimental behavior with a high level of accuracy and also at the first experimental section, temperature levels are predicted in a much more physical manner than steady state data. Such improvements are typical of unsteady simulations, where the mixing of vapor fuel and the turbulent dispersion of spray are more physically predicted, leading more fuel toward the corner recirculation zone where accordingly higher temperatures are determined. However, the flame front position, which can be identified by temperature fluctuations peak values, is slightly overestimated, according to the inability of properly predicting the jet opening angle. Furthermore, some discrepancies in peak values can be recovered for example at $z/R = 1.5$, where scale resolved and RANS results are nearly equal. The fine grid M2 does not show appreciable improvements nor in terms of velocity and temperature profiles, leading to the conclusion that SAS approach is not totally able to represent the physics under investigation and that LES can be suggested as future development to correctly catch the turbulent mixing and flame structure.

However, the overall agreement obtained in the proposed scale resolved framework is satisfactory and comparable with the one reported in previous numerical works [12,18].

Finally, to integrate the comparison between scale resolved and RANS modelling, computational costs should be also considered. Simulations have been carried out using 32 cores of a Linux cluster comprising Intel Haswell 2.40 GHz CPUs. For RANS calculations roughly 768 CPU hours were required, whereas for SAS 7296 CPU hours were needed.

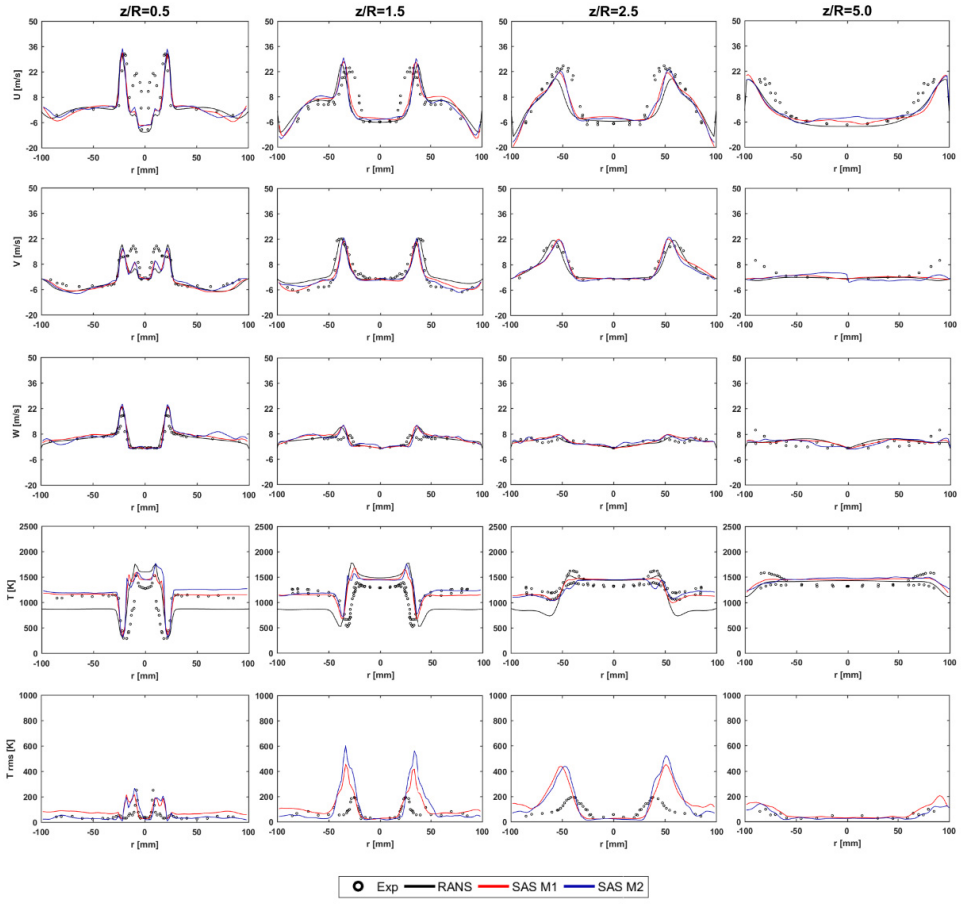

Figure 4: Comparison of velocity, temperature and temperature fluctuations radial profiles of RANS and SAS simulations at several axial distances.

6. Conclusions

In this work, SAS calculations of a swirler stabilized turbulent spray flame fed by Jet A-1 have been performed. The comparison with experimental data show an overall good agreement of the reported scale resolved simulations both in terms of flow field and temperature evolution. SAS has proved to be able to physically represent the unsteady behavior of the flame under investigation leading to important enhancements with respect to RANS results. The remaining discrepancies against experimental data have not been recovered by the proposed mesh refinement, suggesting the exploitation of LES as future development. However, the obtained overall agreement is satisfactory and the numerical setup used in this work could be employed for more complex turbulent spray flames typical of aero-engine combustors.

Acknowledgements

We acknowledge the CINECA award under the ISCRA initiative, for the availability of high performance computing resources and support.

The authors would also like to thank Mattia Berti for the contribution on the preliminary RANS sensitivity during his Master's thesis.

References

[1] Sheen D. Swirl-stabilised turbulent spray flames in an axisymmetric model combustor. PhD Thesis. Imperial College, 1993.
[2] ICAO. Environmental report - Aviation and climate change. 2010.
[3] Gicquel L, Staffelbach G, Poinsot T. Large Eddy Simulations of gaseous flames in gas turbine combustion chambers. Prog Energy Combust Sci 2012;38.
[4] Galpin J, Naudin A, Vervisch L, Angelberger C, Colin O, Domingo P. Large eddy simulation of a fuel lean premixed turbulent swirl-burner. Combust Flame 2008;155:247–66.
[5] Pierce C, Moin P. Progress-variable approach for large-eddy simulation of non-premixed turbulent combustion. J Fluid Mech 2004;504:73–97.
[6] Andreini A, Bianchini C, Innocenti A. Large Eddy Simulation of a Bluff Body Stabilized Lean Premixed Flame. J Combust 2014.
[7] Chrigui M, Gounder J, Sadiki A, Masri A, Janicka J. Partially premixed reacting acetone spray using LES and FGM tabulated chemistry. Combust Flame 2012;159:2718–41.
[8] Andreini A, Bertini D, Facchini B, Puggelli S. Large-eddy simulation of a turbulent spray flame using the flamelet generated manifold approach. Energy Procedia 2015;82:395–401.
[9] Van Oijen J, de Goey L. Modelling of premixed laminar flames using flamelet-generated manifolds. Combust Sci Technol 2000;161:113–37.
[10] Andreini A, Bertini D, Mazzei L, Puggelli S. Assessment of scale resolved CFD methods for the investigation of lean burn spray flames, Proceedings of ASME Turbo Expo 2016, No. GT2016-57143: 2016.
[11] Menter FR, Egorov Y. The Scale-Adaptive Simulation Method for Unsteady Turbulent Flow Predictions. Part 1: Theory and Model Description. Flow Turbul Combust 2010;85:113–38.
[12] Jones WP, Lyra S, Navarro-Martinez S. Numerical investigation of swirling kerosene spray flames using Large Eddy Simulation. Combust Flame 2012;159:1539–61.
[13] Sirjean B, Dame E, Sheen DA, You X-Q, Sung C, Pitsch H, et al. A high-temperature chemical kinetic model of n-alkane oxidation, JetSurF version 1.0 2009.
[14] Morsi SA, Alexander AJ. An investigation of particle trajectories in two-phase flow systems. J Fluid Mech 1972;55:193–208. doi:10.1017/S0022112072001806.
[15] Sazhin SS. Advanced models of fuel droplet heating and evaporation. Prog Energy Combust Sci 2006;32:162–214.
[16] Rachner M. Die Stoffeigenschaften von Kerosin Jet A-1. Technical report 1998.
[17] Sheen H, Chen W, Wu J. Flow patterns for an annular flow over an axisymmetric sudden expansion. J Fluid Mech 1997;350:177–88.
[18] Fossi A, deChamplain A, Paquet B, Kalla S, Bergthorson JM. Scale-Adaptive and Large Eddy Simulations of a Turbulent Spray Flame in a Scaled Swirl-Stabilized Gas Turbine Combustor Using Strained Flamelets, Proceedings of ASME Turbo Expo 2015, No. GT2015-42535: 2015.